'C' TYPE PTFE GASKETS PERFORMANCES IN HIGH PRESSURE SOUR APPLICATIONS

Leonardo Baldassarre
Compressors & Expanders Engineering
Executive Manager & Principal Engineer
GE O&G
Florence, Italy

Marco Pelella
Centrifugal Compressors Engineering
Manager & Senior Engineer
GE O&G
Florence, Italy

Leonardo Baldassarre is currently the Engineering Manager & Principal Engineer for Compressors & Expanders with General Electric Oil & Gas Company, in Florence, Italy. He is responsible for all requisition, and standardization as well as for detailed design of new products for centrifugal compressors, reciprocating compressors and turboexpanders. Dr.Baldassarre began his career with General Electric Nuovo Pignone in 1997. He has worked as Design Engineer, R&D Team Leader for centrifugal compressors in Florence, Product Leader for centrifugal and axial compressors, and Requisition Manager for centrifugal compressors both for Florence and Le Creusot teams. Dr. Baldassarre received a B.S. degree (Mechanical Engineering, 1993) and Ph.D. degree (Mechanical Engineering / Turbomachinery Fluid Dynamics, 1998) from the University of Florence. He has authored or coauthored 20+ technical papers, mostly in the area of fluid dynamic design of 3D transonic impellers, rotating stall, and rotordynamics. He presently holds five patents.

Marco Pelella is Engineering Manager for Centrifugal Compressor LNG and Downstream Applications with GE Oil & Gas in Florence, Italy. He also holds the title of Senior Engineer. His responsibilities include the thermodynamic and rotordynamic study of centrifugal compressors as well as their stress verification and material selection. Mr. Pelella graduated in Mechanical Engineering at University of Naples in 1997. He joined GE in 1999 as Design Engineer in Centrifugal Compressor Requisition team, then he has worked as Requisition Team Leader of integrally geared and pipeline compressors, Requisition Manager in Le Creusot (France) for centrifugal compressors of low and medium pressure in normal and sour services. He presently holds 3 patents.

ABSTRACT

Sealing performance in general in centrifugal compressors and in particular in sour gas applications is extremely important to prevent safety issues and EHS concerns. As known, H_2S starts to become lethal with concentrations in excess of 100 ppm. In general the elastomeric O-ring gaskets (such as FKM-Fluor elastomer or FFKM-Perfluorelastomer), are the most appropriate to guarantee approximately zero leakage towards the environment thanks to their like liquid behavior with very high viscosity.

Unfortunately O-rings are generally quite permeable to gas and have poor mechanical properties in high pressure applications (above 200 bar). If exposed to explosive decompression or extruding forces through the downstream gap between the casing and the head-cover they can deteriorate quickly. This finally leads to sealing performance degradation and compressor shut down.

To avoid the above issues a thermoplastic material such as PTFE-Politetrafluoroetilene (Teflon®) is normally used. PTFE has good mechanical properties, it is not permeable to gas and liquids and consequently it is not affected by explosive decompression. In addition for high pressure application a special profile, generally 'C' shape, is used; a special spring is installed inside the 'C'. This configuration being known as energized gasket.

As plastic materials are only slightly elastic, they cannot rely on their mechanical properties to offer sealing capabilities, as it happens for elastomers, hence PTFE requires a very low surface roughness of the metal parts in touch with it.

During the leakage test of a BCL304/C (design pressure 425barg) an excessive leakage was measured on the inboard gasket ('C' type) with respect to the allowable value, i.e. ~ 700 NmLit/min @ 425 barg versus a requirement of 0.56 NmLit/min (equivalent to 0.01 cm^3/s).

The casing tested and discussed in this paper is barrel compressor architecture with integral head-cover on the casing discharge side and a suction head-cover fixed to the casing by relevant shear rings.

Leakage from the discharge side is self-avoided in such architecture. A leakage recovery system is provided for the suction side. This leakage recovery system is made by 3 different chambers created by 4 gaskets set among the casing and its head-cover.

The first two inboard gaskets (moving from process side to atmospheric side) are PTFE 'C' type and then two elastomeric O-rings are used on the outboard side. During the leakage test the leakage is measured at full pressure across the first 'C' PTFE gasket, by using proper calibrated flow meters. For safety reasons the leakage across the first inboard 'C' gasket has to be guaranteed at very low level (equivalent to 10 bubbles of 1mm^3 volume per second).

Present work reports the activity done to solve the issue of excessive leakage flow detected from the inboard seal.

Design solutions to solve the issue are discussed. Impact of several parameters on final leakage has been analyzed to better assess this phenomena:

    a.   gasket groove geometry (circularity and roughness) and potential damages (scratches, dents, etc.),

    b.   gasket surfaces roughness and potential damages (scratches, dents, etc.),

    c.   gasket-groove assembly and gasket compression including the eccentricity between casing and head-cover causing a non-uniform compression over the 360°.

Since no major defects were found on both grooves and gasket surfaces the main focus of the activity was to assess the impact of reduced gasket compression on leakage flow. A special 1D gas dynamic model has been developed in order to physically relate leakage flow with gas pressure and some other key parameters:

    i.   Thermodynamic conditions,
    ii.   Elasto-plastic material properties,
    iii.   Contact surfaces tribological characteristics.
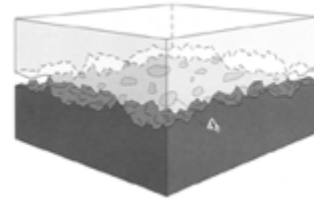
The model is validated through tests on the real compressor going from 0 to full pressure (425 barg) using nitrogen gas.

Finally the root cause of the excessive leakage was understood and the gasket design changed. This allowed to fully meet the very tight contractual requirements even with significant margins vs. max allowable values. The robustness of the new design was confirmed with three repetitions of the tests and by using spares gaskets with same design.

Moreover, the impact of the groove surface roughness was tested using the new gasket design and comparing the results with two different roughness values Ra=0,4μm and Ra=0,8μm. These results are of capital importance to assess the sensitivity of the configuration to possible deterioration of the surfaces.

1. INTRODUCTION

The sealing performance in sour application is extremely important in centrifugal compressor design to prevent any safety issue to the environment, being H_2S a lethal gas starting from concentration of 100 ppm.

In general the elastomeric O-ring gaskets (such as FKM-Fluor elastomer or FFKM-Perfluorelastomer), are the best to guarantee approximately zero leakage towards the external since they behave as liquids with very high viscosity.

When installed in the groove the O-ring is constrained by the surrounding walls which finally squeezes it and, thanks to its elasticity and softness, it can even compensate mating components defects and out of spec. surface roughness.

O-rings are generally quite permeable to gas and have poor mechanical properties in high pressure applications (above 200 bar). O-ring is porous so when subjected to pressure and in particular in presence of relatively "small" molecules like CO_2, it tends to be filled with gas at high pressure. If pressure is quickly reduced these molecules tend to remain entrapped in the O-ring finally trying to create their path to escape to the lower pressure environment. This creates damages to the O-ring in the form of bubbles, blistering, cracks etc. (see Figure 1.) making the O-ring losing the capability to seal the component. In presence of high pressures (even without explosive decompression) the O-ring tends to deform finally experiencing extrusion issues and again losing the capability to properly seal the downstream gap. .

Figure 1. Damaged O-ring caused by explosive decompression

To avoid the above issues a thermoplastic material such as PTFE-Politetrafluoroetilene (Teflon®) is normally used. PTFE has, good mechanical properties, is not permeable to gas and liquids, and consequently is not affected by explosive decompression. In addition for high pressure application a special profile, generally a 'C' shape, is used; inside the 'C' a spring is installed (see Figure 2.).

Figure 2. 'C' gasket schematic

As plastic materials are only slightly elastic, they cannot rely on their mechanical properties to offer sealing capabilities, as it happens for elastomers.
'C' gaskets are energized by the spring at low pressure and by the gas itself at higher pressures. The effect of both spring and gas pressure is to push the lips against the surfaces to be sealed (see Figure 3.). PTFE rings can hardly accommodate for surface scratches and they require a very low surface roughness.
When the gas pressure is very high, the gasket is coupled with a back-up ring.
Under the force of gas pressure the 'C' gaskets, without back up ring, could be pushed into the downstream gap, giving place to gasket extrusion. The back-up ring closes the gap and avoids extrusion.
The back-up ring is made of plastic resistant material, such as PEEK (Polyether ether ketone).
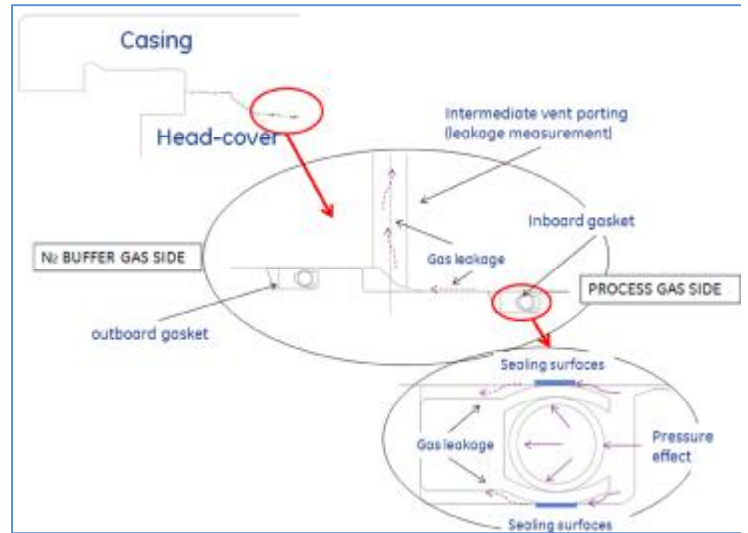
Figure 3. 'C' gasket arrangement & sealing mechanism

The casing tested and discussed in this paper is barrel compressor architecture with integral head-cover on the casing discharge side and a suction head-cover fixed to the casing by relevant shear rings (see Figure 4a-b).

Figure 4a. Leakage test arrangement of high pressure barrel compressor
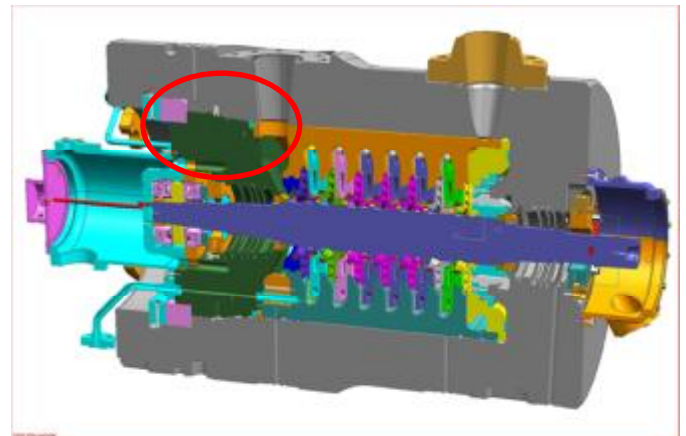

Figure 4b. Sectional view of high pressure barrel compressor

As the leakage from the discharge side is avoided in such architecture, a leakage recovery system is provided for the suction side. This leakage recovery system is made by 3 different chambers created by 4 gaskets set among the casing and its head-cover (see Figure 4c.).
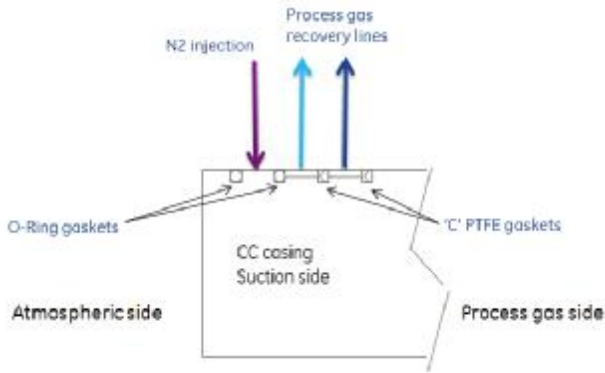

Figure 4c. Leakage recovery system schematic

The first two inboard gaskets (moving from process side to atmospheric side) are PTFE 'C' type and then two elastomeric O-rings are used on the outboard side. During the leakage test the leakage is measured across the first 'C' PTFE gasket at full pressure (see Figure 3.) by using proper calibrated flow meters, and then, through a bubble soap test, is checked for any leakage towards the external by pressurizing with Nitrogen at 7 bar the third chamber made by two O-rings (see Figure 4c.). For safety reasons the leakage across the first inboard 'C' gasket has to be guaranteed at very low level (equivalent to 10 bubbles of 1mm^3 volume per second).

The present work reports the activity done to solve the issue of excessive leakage flow from the inboard seal considering the impact of key parameters on the phenomenon.

2. ISSUES DESCRIPTION AND ROOT CAUSE ANALYSIS

During the leakage test of the BCL304/C an excessive leakage through the inboard 'C' gasket was measured ~700 NmLit/min @ 425bar versus a required value of 0.56 NmLit/min (equivalent to 0.01 cm^3/s).

This leakage is normally rooted to the atmosphere during the test (being the test gas nitrogen) and no leakage was observed through the outboard O-ring on which a max pressure of 7 bar was acting.

The leakage measurements through the inboard 'C' gasket, from low pressure up to design pressure, are reported in the Graph 1 indicated as "1st test std gaskets".
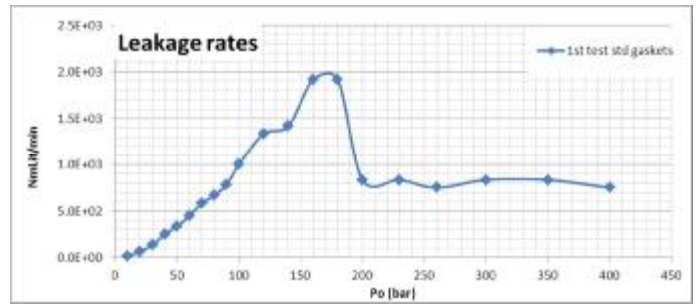
Graph 1. Leakage test results:1st test with standard 'C' gaskets design and standard PTFE material

In order to figure out the root cause of the issue an extensive measurement campaign was conducted to check the impact of the key parameters that have an influence in the physical phenomenon:

    a.   gasket groove geometry (circularity and roughness) and potential damages (scratches, dents, etc.):

No scratches, dents or macroscopic defects were found on the contact surfaces.

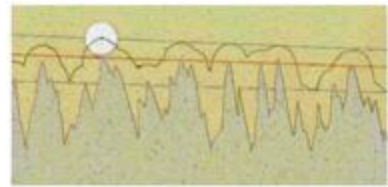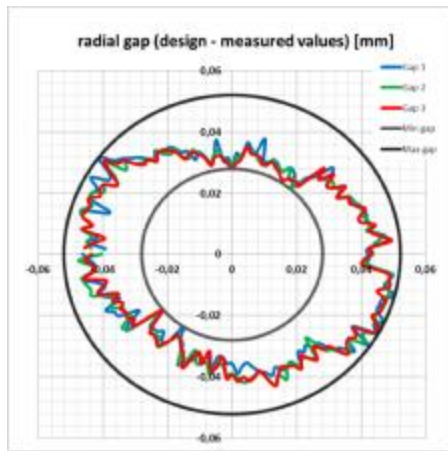The surfaces roughness Ra values were found within design values

Figure 5. Roughness profile as traced by the contact probe on the real surface profile.

The circularity values were taken each 2.5°; the relevant results are showed in the graph 2a-b and the max difference between design and measured radial values were in the order of 0.04÷0.06 mm leading to a gasket groove height higher than max design value ->*first finding*
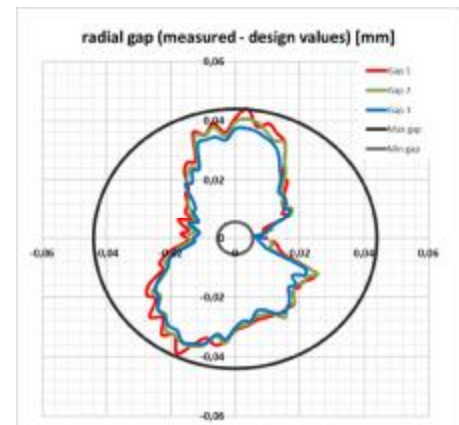
Graph 2a. Casing circularity measurement

Graph 2b. Head-cover circularity measurement

b. gasket surfaces roughness and potential damages (scratches, dents, etc.):

No scratches, dents or macroscopic defects were found on the contact surfaces.

the roughness of the gasket material was found above 1μm (above the expected value)-> *second finding*

c. the gasket-groove assembly:
the casing/head-cover eccentricity (once the parts are assembled) has been considered. This produces a groove height not uniform in the 360°, causing a non-uniform gasket compression over the 360° (minimum on the top vertical position and a maximum on the bottom side).

From the casing/head-cover eccentricity measurement appeared that the gasket compression on the top vertical position (0.4mm) was out of the min design allowable value -> *third finding*.

From the above findings two actionable areas were identified:

1. Check the impact of a different material with improved surface properties (to address the finding in item b). This topic will be analyzed in section 3.
2. Check the impact of reduced gasket compression on the gasket contact pressure and length (to address the findings in items a and c). This topic will be analyzed in detail on section 4 characterizing the leakage flow with gas pressure and sealing contact surfaces tribological aspects using an ad hoc gas dynamic model.

3. IMPACT OF DIFFERENT JACKET MATERIAL ON SEALING PERFORMANCES

The 1st test was done using pure PTFE 'C' gaskets, but PTFE can be modified by incorporating different fillers in order to increase key properties for tribological applications such as hardness, modulus, compression strength, thermal conductivity as well as resistance to wear and surface roughness. Commonly used fiber reinforcements are short glass and carbon fibres. They strongly enhance the wear resistance and reduce creep compared to pure PTFE. Particle reinforcements are often done by polymer particles, i.e. polyphenylene-sulphide (PPS), polyimide (PI), PEEK and graphite. Metal powder, especially bronze, provides high load-bearing capability, very low wear rates and good frictional coefficients. Figure 6 gives an example of PTFE matrix filled with different materials.
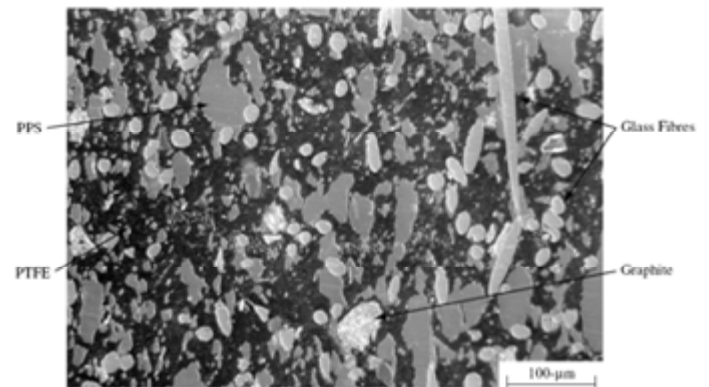

Figure 6. Example of PTFE matrix filled with different materials.

To guarantee optimal sealing performances the PTFE is modified to incorporate a perfluoropropyl-vinyl-ether (PPVE) modifier (see Figure 7.), the same chemical modifier used for the PFA (melt-processable fluorothermoplastic). However the modifier content is less than 1%, for this reason it can be still classified as PTFE homopolymer, successfully introducing part of the property profile of PFA (mechanical properties and improved surface roughness) into PTFE without losing the typical properties of conventional PTFE (typically the chemical resistance).
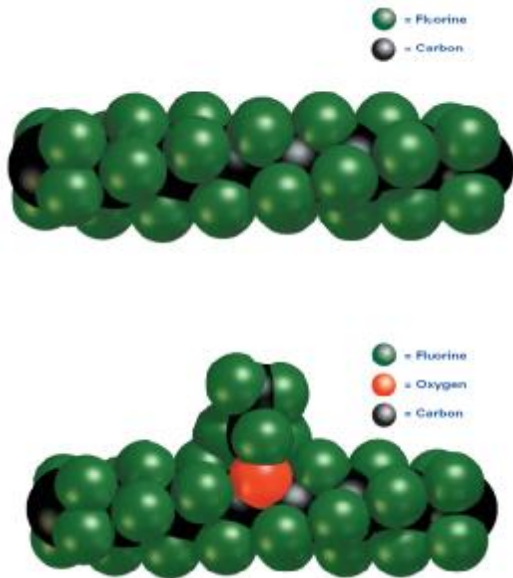
Figure 7. Structure difference between pure PTFE and modified PTFE

The figures 8a-b show the surface roughness improvement between conventional PTFE (Figure 8a.) and the modified one (Figure 8b.). In addition the lower melt viscosity leads to better particles fusion during sintering, as a result a denser polymer structure with lower permeability is obtained reducing the void content by a factor of ~ 2:1. The Figures 9a-b show the difference between the modified and un-modified PTFE matrix as relieved by microscopic investigations (Figure 9b shows that the boundary of the second particles present in Figure 9a have disappeared).

Figure 8a. Conventional PTFE   *Figure 8b. Modified PTFE*
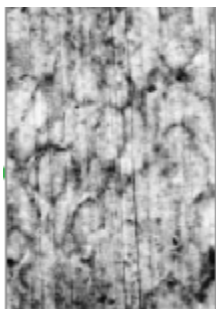
Figure 9a. Conventional PTFE   *Figure 9b. Modified PTFE*
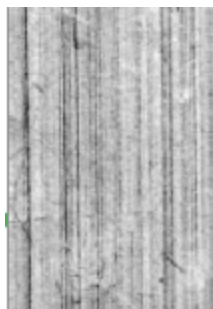
The effect of the improved material (lower roughness and gas permeability) was investigated making a 2nd test with original gasket design and a material able to achieve Ra value of 0.1÷0.3µm. The gasket groove geometry was kept identical to the one of the 1st test.

The results of the 2nd test are showed in the graph 3 indicated as "2nd test std gaskets".
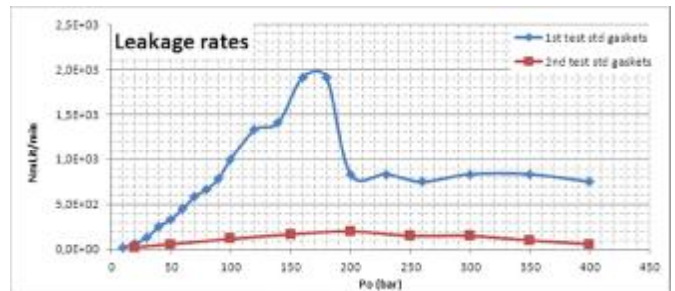
Graph 3. Leakage test comparison:1st test with standard 'C' gaskets design and standard PTFE material; 2nd test with standard 'C' gaskets design and modified PTFE material

The graph 3 shows that the 2nd gasket material performs much better that the first one, allowing reducing the leakage rate of more than one order of magnitude.

The leakage rate was still above the max allowable required, and since no macroscopic defects were found able to explain the test deviation from expected value, it was decided to go deep in the investigation of microscopic aspects of the issue and an analytical model was developed as explained in the section 4.

4. IMPACT OF GASKET COMPRESSION ON SEALING PERFORMANCE – *LEAKAGE GAS DYNAMIC MODEL*

In order to link the leakage rate with the contact surfaces micro-characteristics, an efflux gas dynamic model was developed that puts in relation the test pressure, the leakage flow and the surface asperities.

The basic idea about the possible gas passage area is that the contact between the gasket and groove surfaces (on both casing and head-cover) is not perfect as shown in the Figures 10, leaving micro-holes all around the 360° due to the asperities contacts.
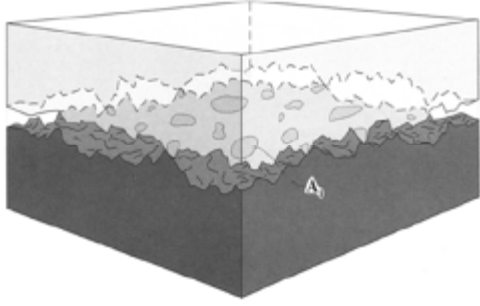
Figure 10. Real contact area of rough surfaces in contact; A_r, is the true area of contact, i.e. $A_r = \sum_{i=1}^{n} A_i$, n is the number of asperities (Stachowiak G. W. and Batchelor A.W., (2005), Engineering Tribology 3°ed., Burlington: Elsevier Butterworth-Heinemann).

The additional simplification done by the authors is that these contacts create micro-tubes for gas passage and the relevant gas dynamics across them is analyzed with the one-dimensional friction model using the Fanno theory.

More in details, the equivalent model is constituted by a gas reservoir (the casing itself) at test pressure (p_0) connected with several micro-tubes, later on called capillaries, working in parallel, with length less or equal to the gasket lip length and discharging at atmosphere (p_3) (see scheme 1)
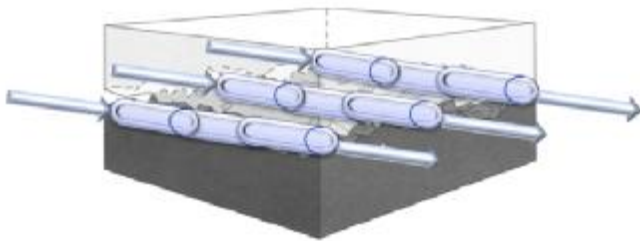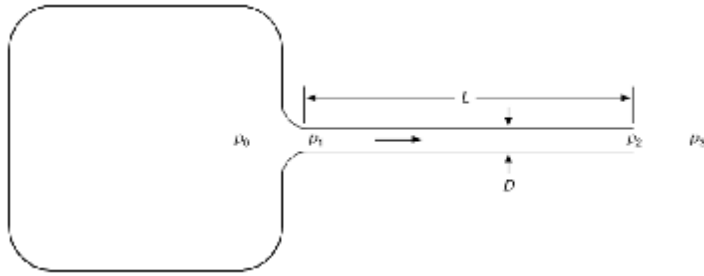
Scheme 1. Capillary model

Considering that D (capillary diameter) and n_c (number of capillaries) are the two unknown to be found, the calculation for the single capillary is done using the equations of the one-dimensional flow across a tube with friction (Fanno theory) preceded by a reservoir equipped with discharging isentropic nozzles.

Starting from the basic equation of:

$$G_{tot} = G \cdot n_c \qquad (1)$$

It is possible to rearrange it, writing:

$$G_{tot} = \frac{pD^2 n_c p_0 \Psi}{4a_0} \qquad (2)$$

where

$$\Psi = \sqrt{\frac{2k^2}{k-1}\left(\frac{p_1}{p_0}\right)^{\frac{2}{k}}\left(1-\left(\frac{p_1}{p_0}\right)^{\frac{k-1}{k}}\right)} \qquad (3)$$

Ψ is called the discharge coefficient. For a graphical representation of the above parameter see Appendix B.

To calculate Ψ, first it is needed to calculate the ratio p_1/p_0 knowing the inlet Mach number (M_1).
M_1 can be derived by using the equation:

$$\frac{4fL_{max}}{D} = \frac{1-M_1^2}{kM_1^2} + \frac{k+1}{2k}\ln\left(\frac{\frac{k+1}{2}M_1^2}{1+\frac{k-1}{2}M_1^2}\right) \qquad (4)$$

Note:
a) for $M_1 < 0.24$ a best fitting is given by equation
$$M_1 = C \cdot N^{-B} \qquad (5)$$
where C=0.776191; B=0.492760.

b) Flow regime is assumed to be laminar, hence f=64/Re.

From M_1 is then calculated the ratio p_0/p_1 with equation:

$$\frac{p_0}{p_1} = \left(1+\left(\frac{k-1}{2}\right)M_1^2\right)^{\frac{k}{k-1}} \qquad (6)$$

From eq. 2 it is possible to calculate the capillary diameter D knowing n_c, being G_{tot} a measured value.

To calculate n_c the following equations are used:

$$p_2 = \frac{p_2}{p_1}\frac{p_1}{p_0}p_0 \qquad (7)$$

$$\frac{p_2}{p_1} = \frac{1}{M_1}\sqrt{\frac{k+1}{2+(k-1)M_1^2}} \qquad (8)$$

and relation of M_1 with N can be rearranged as follows:

$$M_1 = C\left(\frac{4 \cdot 64_e L}{R_e D}\right)^{-B} \quad \rightarrow \quad M_1 = C\left(\frac{p\,64 n_c\, \boldsymbol{m} L}{G_{tot}}\right)^{-B} \quad (9)$$

Hence, by iterative way, n_c can be calculated matching $p_2 = p_3$, and knowing all the other parameters in the eq. 9

From a theoretical standpoint the above approach is valid only for sonic discharge conditions that match the atmospheric pressure, as consequence it means calculating the minimum capillary size D because Ψ is maximum in sonic conditions (see Appendix B). To be noted that for the purpose of the present work the flow condition where $M_2 = 1$ and $p_2 > p_3$ will be not considered. This is relevant to chocking flow where the Kutta condition is not respected, i.e. an expansion shock wave is present at the exit of capillary.

In addition below 100 bar D and n_c are kept constant and equal to the values found at gas pressure immediately above.
This is based on the fact that D and n_c are linked to the contact pressure of the mating surfaces produced by the gasket spring exerted on the gasket lips. FEA calculation provides an average contact pressure of $50 \div 100$ bar (see Figure11a.).
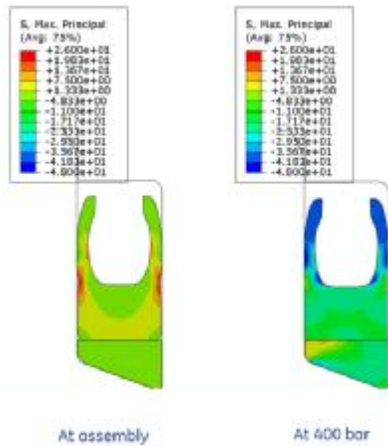Finally also the contact length of the sealing surfaces L is calculated using FEA (see Figure11b.).
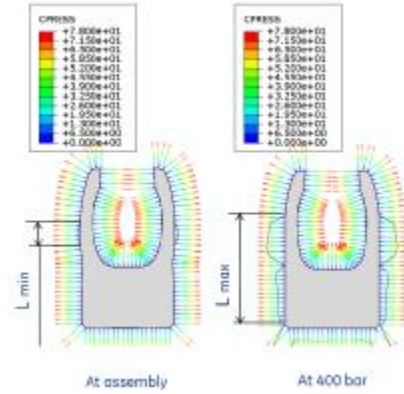

Figure11a. Gasket stress analysis.

Figure 11b. Gasket contact length analysis.

The table 1a and the graph 4a show the model results relevant to the 1st leakage test, while table 1b and graph 4b show the ones relevant to 2nd leakage test.

Table 1a. 1st test results

| Gtot (kg/s)	p0 (bar)	nc	D (m⁻⁶)	Atot (m⁻¹²)	L (mm)	Re	Y	N
1.39E-06	20.00	1.9E+04	2.32	78915	0.9	2	3.1E-03	4.59E+04
6.94E-06	50.00	1.9E+04	2.32	78915	2.0	10	6.1E-03	2.16E+04
1.63E-05	90.00	1.9E+04	2.32	78915	4.1	24	8.0E-03	1.88E+04
3.47E-05	150.00	1.9E+04	2.32	78915	6.0	51	1.0E-02	1.30E+04
1.63E-05	245.00	2.4E+04	1.42	36977	6.0	31	6.3E-03	3.48E+04
1.74E-05	350.00	5.2E+04	0.98	39518	6.0	22	4.4E-03	7.24E+04
1.56E-05	400.00	6.1E+04	0.86	35538	6.0	19	3.8E-03	9.48E+04

Table 1b. 2nd test results

Gtot (kg/s)	p0 (bar)	nc	D (m⁻⁶)	A_{tot} (m⁻¹²)	L (mm)	Re	Y	N
5,23E-07	20,00	1,9E+03	2,32	7903	0,9	8	1,2E-02	1,22E+04
1,21E-06	50,00	1,9E+03	2,32	7903	2,0	18	1,1E-02	1,24E+04
2,45E-06	100,00	1,9E+03	2,32	7903	4,1	36	1,1E-02	1,26E+04
3,47E-06	150,00	1,9E+03	2,32	7903	6,0	51	1,0E-02	1,30E+04
3,12E-06	250,00	4,7E+03	1,38	7109	6,0	30	6,1E-03	3,65E+04
2,60E-06	325,00	6,7E+03	1,06	5924	6,0	23	4,7E-03	6,22E+04
1,21E-06	400,00	4,8E+03	0,86	2764	6,0	19	3,8E-03	9,48E+04
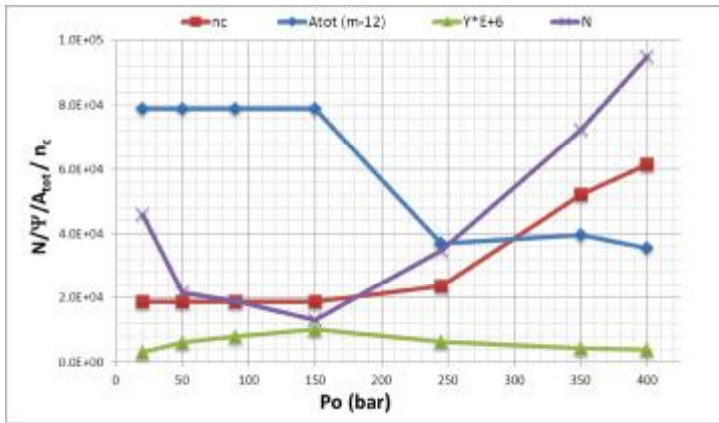
*Graph 4a. 1st test N, Y, A_{tot} and n_c trends varying casing test pressure.*
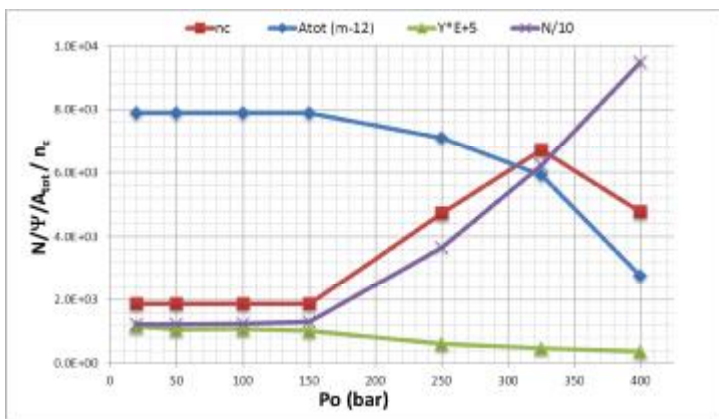
Graph 4b. 2nd test N, Y, A_{tot} and n_c trends varying casing test pressure.

From the above results the following considerations arise:

a) The number of capillaries n_c found for the 2nd test is one order of magnitude less than 1st test n_c, that in turns means that the reduction of n_c is proportional to the reduction of the leakage rates, being the size D remained unchanged. The fact that D is invariant between the two tests is due to the gas dynamic model used and relevant assumptions of sonic discharge condition with $p_2=p_3$.

b) Above 250 bar the flow passage areas A_{tot} in the 2nd test tends to decrease with gas pressure while the same doesn't happen in the 1st test. This can be explained considering that the first settling of parameters D, n_c and L_{min}, produced by the gasket spring at assembly (better in the 2nd test than 1st one) is vital to achieve the target sealing performance. In other terms, if the gasket is not able to properly seal the groove surfaces at the assembly then the gas will flow in between the gasket lip and the groove surfaces and the gas pressure will be distributed both on the internal and external side of the 'C' gasket lips producing a sort of

force balancing on the two sides of the lip preventing it to adhere properly to the groove surface. For this reason A_{tot} and n_c in the 1st test continuously increase with p_0, while in the 2nd test the gas pressure results more effective in pushing the gasket lip toward the groove surfaces causing the reduction of A_{tot} and n_c while p_0 increases.

c) Considering to put in succession the calculated n_c at low pressure (<100bar) along the groove circumference, it is possible to calculate an arc of not perfect sealing of ∼40mm in the 1st test and ∼4mm in the 2nd test. These arcs can be considered located on the top vertical position of the gaskets-groove assembly where the gasket compression is the minimum and the metal-gasket contact tends to be less effective (see scheme 2).
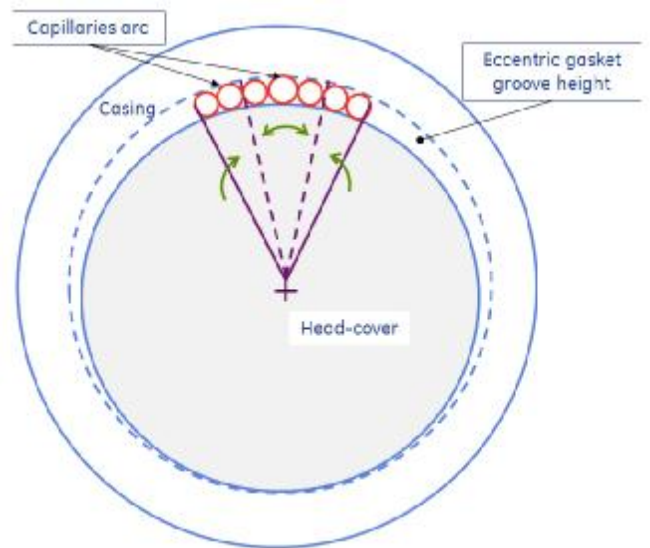
Scheme 2. Capillaries arc located on the top vertical position of the casing head-cover assembly where the gasket groove height is max.

d) The calculated size of the capillaries D indicates that it is unlikely to relate the excessive flow rate to a surface macro-defects being their size in the order of microns, hence the issue of excessive leakage has to be related to the micro-openings left at the mating sealing surfaces by their micro-asperities.

Considering the 2nd test, above 150 bar the flow rate starts to decrease, while n_c increase, D decreases and A_{tot} decrease too, showing physical consistency with the fact that as p_0 increases the internal pressure on the gasket lips increase compressing more and more the gasket material into the hardware asperities reducing the passage area for the gas leakage. In addition as the hardware surface asperities have a fractal topography (see Figure 12a - Stachowiak G. W. and Batchelor A.W., (2005), *Engineering Tribology 3°ed.,* Burlington: Elsevier Butterworth-Heinemann.), it is quite consistent that their number increases with pressure (n_c increase) since the gasket material progresses yielded in the hardware asperities and it is also consistent that the equivalent D has to be reduced (see Figure12b.). From the contact theory of the rough surfaces it is understood that the

number of asperities in contact increases proportionally with the applied contact load (see Figure 12b). This is true both in elastic and plastic condition if the height distribution of the surfaces is close to a Gaussian one (see Figure 12c - Johnson K.L., (1985), Contact Mechanics, Cambridge: University Press).

e) In the 2nd test it is observed that n_c starts to decrease above 325bar while in the 1st test it progressively continues to increase with pressure. This can be related to improved gasket material used in the 2nd test that is able to better adapt itself to the micro-asperities of metal surfaces, producing, above a certain pressure, a contemporary reduction of both D and n_c that leads to have a more significant reduction of A_{tot}.
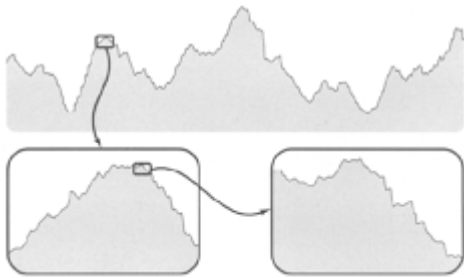

Figure 12a. Fractal structure of real surfaces.

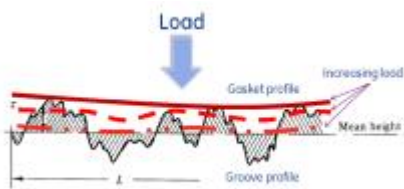

Figure 12b. Gasket-groove contact schematic: increasing load increases the number of asperities in contact, hence n_c is increased and D is reduced.
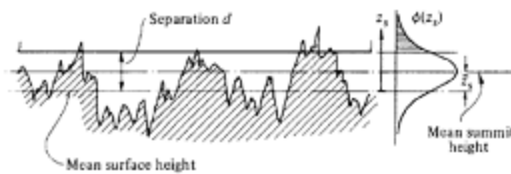

Figure 12c. Contact of a randomly rough surface with a smooth flat

5. IMPACT OF GASKET OVERSIZING ON SEALING PERFORMANCES AND ISSUE RESOLUTION.

From the analysis done in section 4 it comes out that in order to fix the issue the arc of capillaries located on the top vertical position of the gasket-groove mating surface needs to be reduced. In addition, the proposed gas dynamic model shows that a small reduction of D and n_c produces a significant impact on leakage flow (please refer to appendix A eq.11 to have a direct relation between G and D, i.e. 4th power dependence). In order to address the findings in section 2-item a and c, new gasket geometry was studied with the selected supplier. The aim of this change was to maximize residual gasket compression at assembly to a maximum value sustainable by the gasket spring. A new gasket was manufactured with increased height to be installed in the same groove. FEA was carried out on the gasket-groove assembly in order to define and optimize the new contact pressure and the new contact length values for the actual groove geometry (see Figure13.).
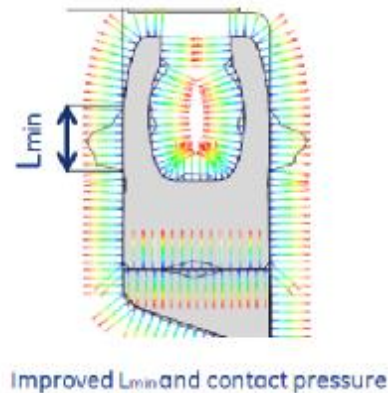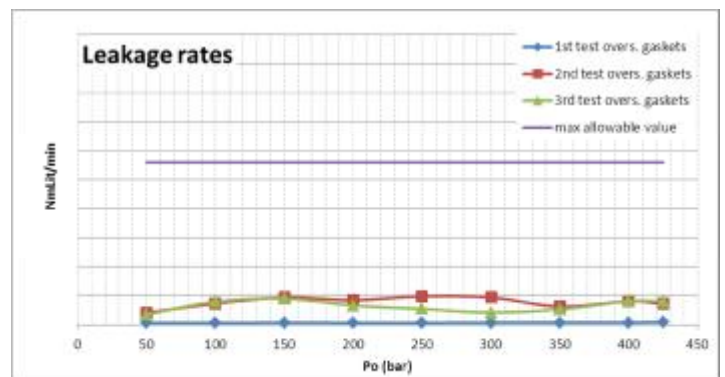

Figure 13. Improved gasket contact length analysis.

The first test with oversized gasket was successful and it was repeated two more times. The additional tests were all positively passed with measured leakage rates well below the acceptance level. A demonstration of the robustness of the new gasket design is shown on graph 5.

Graph 5. Leakage test results with oversized gaskets

By applying the capillary gas dynamic model to the successful tests with oversized gaskets a number of capillaries below 1

was calculated, i..e solution didn't appear to be physical. Nevertheless it can be seen as qualitative indication of the strong reduction of the number of capillaries. The arc collapsed from a length of few millimeters to a length of some microns thanks to the increased gasket compression (oversized height design).

By having reached the limit of the proposed gas dynamic model, it means that that the Knudsen number K_n (as ratio of the molecular mean free path λ and D) is approaching values greater than 10^{-3}, hence the flow is in the regime of the slip and transitional flow (see Appendix C) where micro-fluidic models have to be applies to find correlation among flow, Δp and surface micro-geometries that is out of the scope of the present work.

It also appears that G_{tot} has no variation with p_0, i.e. (eq. 2) p_0 is in inverse proportion with the product of Ψ, D and n_c, that in turn means the effective A_{tot} given by $\Psi*A_{tot}$, (a_0 is assumed constant).

Since the leakage flow remains at low level from low pressure up to 425 bar the same consideration of section 4 part b can be recalled regarding the importance of the first settling of parameters D, n_c and L_{min} at the assembly.

5. IMPACT OF GROOVE ROUGHNESS ON GASKET SEALING PERFORMANCE

After the issue resolution a new test campaign was carried out on a different compressor (same size and pressure rating) with oversized gaskets and increased groove surface roughness.

The graph 6 reports the result of the new test campaign (Ra=0,8 μm of groove surface) and compares it with the previous test (Ra=0,4 μm of groove surface), showing also the respective max allowable limits.
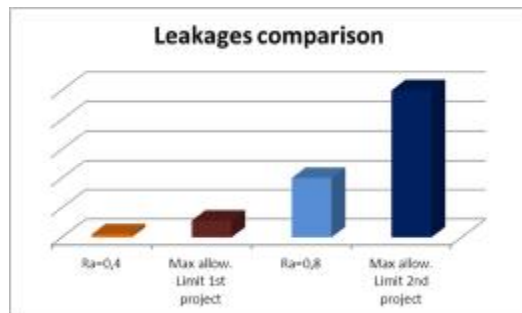
Graph 6. Leakage rate comparison at different groove surface roughness

The above results from one side highlight the impact of the groove roughness on the sealing performance, from the other side confirm the goodness of the oversized gasket design that, even with not optimized groove roughness, is capable to keep the leakage within acceptable levels.

In addition another consideration is possible to derive from the above results, i.e. it is possible to apply a less expensive machining operation on both casing and head-cover passing from Ra=0,4 to 0,8μm (more easy to obtain with standard manufacturing operations) provided that new oversized gasket design is implemented.

6. CONCLUSION

The present work reports the activity done to solve the issue of excessive leakage flow from the inboard seal where no major defects were found on both gasket and groove surfaces.
An attempt to correlate the PTFE gasket performances (leakage rate vs. test pressure) with the physical aspects involved in the phenomenon is presented, providing a simplified analytical model that involves the following topics:

- Gas-dynamic,
- Elasto-Plastic material properties,
- Contact surfaces tribological characteristics,

The proposed model represents a step ahead to what is normally done in the industrial practice. In general leakage rate is correlated with an equivalent sonic orifice diameter that in this case appeared a too much simplified model only applicable to macroscopic surface defects.
The proposed model allows a more accurate prediction thus supporting design actions to improve the sealing
The key design parameters, both for gasket and relevant groove, are highlighted:

- gasket geometry, material and roughness,
- gasket groove geometry and roughness.
- gasket residual compression, that in turns means choosing the optimum contact pressure and contact length.

The test results validated the gas dynamic model predictability and also its range of applicability. Thanks to the new theoretical approach extremely low leakages (below 0.01 cm^3/s) were achieved that indeed are of capital importance in high pressure-high H$_2$S service. The evidence of the goodness of the new design was demonstrated through repeated successful tests on a real compressor BCL304/C (design pressure 425 barg).

In addition the present work highlights the importance of specifying new parameters in the gasket purchase specification that in the standard practice are normally not considered such as the oversizing of the 'C' height to obtain the optimum contact pressure and length requiring dedicated FE analysis.

Finally the new oversized gasket design was also tested with different groove surface roughness, comparing the results of Ra=0,4 and Ra=0,8μm. It allows a less expensive machining operation on both casing and head-covers (since Ra=0,8μm is easier to obtain with standard manufacturing operations) if the contractual requirements in terms of leakage rates permit it.

NOMENCLATURE

G= capillary mass flow [kg/s]
G_{tot}= total leakage mass flow [kg/s]
A= capillary cross section, [m2]
D= capillary equivalent diameter [m]
L= capillary length [m]
n_c= total number of capillaries
f= friction factor
Ψ= discharge coefficient, (represented as G/G0 in Appendix B)
p_0= reservoir absolute pressure [Pa]
$p_3$0 atmospheric pressure [Pa]
p_{1-2}= absolute pressures at inlet and outlet of capillary tube [Pa]
p_m0 arithmetic mean of absolute pressures [Pa]
k= ratio of specific heats
z= gas compressibility
Mw= molecular weight [kg/mol]
M_1= Mach number at capillary inlet
M_2= Mach number at capillary outlet
N= Fanno resistance coefficient=4fL/D
R= gas constant [J*K-1*mol-1]
μ0 gas dynamic viscosity [Pa*s]
a_0= speed of sound at reservoir conditions [m/s].

FEA= finite element analysis
EHS= environment, health and safety
H_2S= hydrogen sulfide
CO_2= carbon dioxide

APPENDIX A

Other two expressions can be utilized for calculating the mass flow of gases flowing through micro-openings (valid for D from 0.005 to 0.06 mm) [Schwartzberg and Gurevich - Am. Inst. Chem. Eng. J., 16, 762 -766 (1970)],
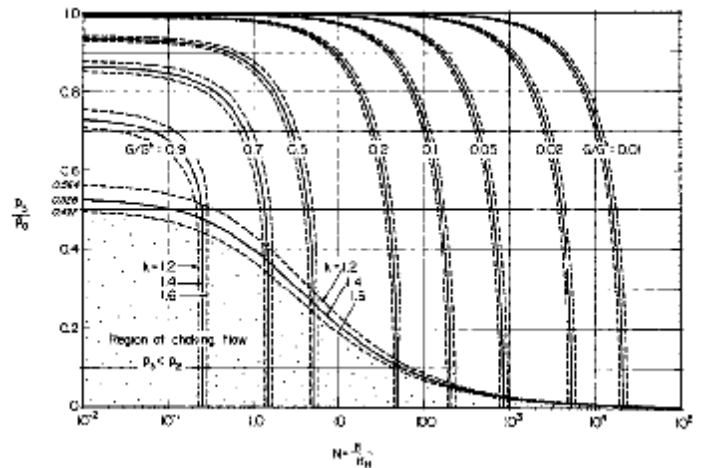
$$G = \left(p_1{}^2 - p_2{}^2\right)\frac{M_w AD}{8mRT_0}\frac{1}{\left[\frac{8L}{D} + \frac{R_\varepsilon}{3}\ln\left(\frac{p_1}{p_2}\right)\right]} \tag{10}$$

or the simpler Poiseuille law (basis for all the capillary flow at low Re for incompressible fluid - i.e. $M_1 \ll 1$)

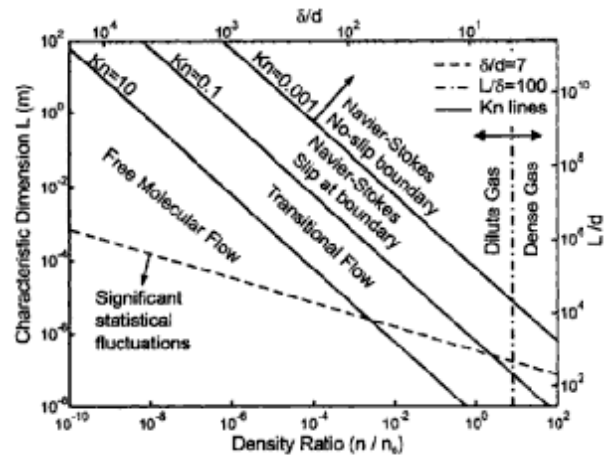$$G = \frac{rp(p_1 - p_2)D^4}{(128mL)} \tag{11}$$

Both equation 10 and 11 are in good agreement with flow calculated using the proposed gas dynamic model.

APPENDIX B

Design chart for adiabatic flow with friction in ducts (Perry R.H., Green Don W., (1984), *Perry's Chemical engineers' handbook 6th ed.,* Mc Graw-Hill Book Co,*)*

APPENDIX C

Flow regime chart in function of dimensionaless quantities (Nguyen Nam-Trung, Wereely S.T., (2002), *Fundamentals and Applications of Microfluidics,* Norwood: Artech House, Inc.)

$$X = \sqrt{\frac{8}{p}}\frac{l}{D} = \frac{2m}{p_m D}\sqrt{\frac{RT_0}{M_w}}$$

Note: for practical purposes slip flow regime is considered when X is in between 0,014 and 0,1 (Perry R.H., Green Don W., (1984), *Perry's Chemical engineers' handbook 6th ed.,* Mc Graw-Hill Book Co.)

References:

Bayer R.G. (2004) – *Mechanical wear fundamentals and testings 2nd ed.*, New York: Marcel Dakker, Inc.

Carlomagno G.M., (2009)– *Elementi di Gasdinamica,* Naples, Italy: Liguori Editore.

Dyneon (a 3M Company) official web site: *http://solutions.3m.com/wps/portal/3M/en_US/dyneon_fluoropolymers/Home/.*

Johnson K.L., (1985), *Contact Mechanics,* Cambridge: University Press.

Kleinstreuer C., (2009), *Modern Fluid Dyanamic, Basic Theory and Selected Applications in Macro- and Micro-Fluidics,* Springer.

Nguyen Nam-Trung, Wereely S.T., (2002), *Fundamentals and Applications of Microfluidics,* Norwood: Artech House, Inc.

Perry R.H., Green Don W., (1984), *Perry's Chemical engineers' handbook 6th ed.,* Mc Graw-Hill Book Co.

Stachowiak G. W. and Batchelor A.W., (2005), *Engineering Tribology 3°ed.,* Burlington: Elsevier Butterworth-Heinemann.

Stachowiak G.W. (editor), (2005) – *Wear – Materials, Mechanisms and Practice*, Chinchester, England: John Wiley & Sons Ltd.

Acknowledgments: